Mesopotamian journal of Big Data
Vol. **(2025)**, 2025, **pp.** 156–177
DOI: https://doi.org/10.58496/MJBD/2025/011 , ISSN: 2958-6453
https://mesopotamian.press/journals/index.php/BigData

Research Article

Hybrid Quantum-Assisted Deep Learning Model for Early-Stage Alzheimer's Disease Classification Based on MRI Images

Eman A. Radhi [1,*], Mohammed Y. Kamil [1], Mazin Abed Mohammed [2,3]

1 College of Science, Mustansiriyah University, Baghdad, Iraq
2 Department of Artificial Intelligence, College of Computer Science and Information Technology, University of Anbar, Anbar, Iraq
3 College of science, Al-Farabi University, Baghdad, Iraq

ARTICLE INFO

Article History

Received 19 Jan 2025
Revised 21 Jul 2025
Accepted 20 Aug 2025
Published 30 Aug 2025

Keywords

Alzheimer's disease
Quantum machine learning
Medical image classification
Quantum Fourier transform
Hybrid neural networks

ABSTRACT

Alzheimer's disease (AD) presents significant diagnostic challenges owing to the subtle morphological similarities observed in the early stages, with traditional deep learning approaches often struggling to distinguish between the various stages of disease progression via structural Magnetic Resonance Imaging (MRI) data. Quantum computing offers unique advantages for medical image analysis, leveraging superposition and entanglement capabilities to process high-dimensional feature spaces beyond the limits of classical computation. This study introduces a hybrid quantum-classical neural network architecture (HQC-Net) for accurate four-class Alzheimer's disease classification, which uses quantum processing to detect patterns that are often invisible to classical spatial analysis methods. The proposed framework integrates classical feature extractors, including a custom CNN and modified ResNet18, with six-qubit variational quantum circuits that employ multiaxis rotation encoding (RY→RZ→RX), a quantum Fourier transform for spectral decomposition, and multihead attention for effective quantum-classical feature fusion. Comprehensive evaluations were conducted on the Kaggle dataset (5,121 samples) and the OASIS dataset (20,000 samples), incorporating realistic quantum noise modelling, including depolarising, amplitude damping, and phase damping channels. The modified QResNet18 configuration achieved a test accuracy of 99.67%, with perfect discriminative capability (AUC = 1.0000) on the OASIS dataset. Quantum processing demonstrated superior detection of very mild dementia (99.86% accuracy), which is crucial for early intervention. The proposed approach outperformed existing quantum-enhanced methods by 3.57 percentage points while effectively handling the increased diagnostic complexity associated with four-class classification. This study demonstrates a practical quantum advantage for multiclass neuroimaging classification, achieving superior diagnostic accuracy while maintaining computational efficiency and clinical deployment feasibility under current Noisy Intermediate-Scale Quantum (NISQ) hardware constraints.

1. INTRODUCTION

Alzheimer's disease (AD) is the most prevalent neurodegenerative disorder and the leading cause of dementia globally, affecting more than 55 million people. This number is projected to triple by 2050 due to the global increase in life expectancy and the aging population [1]. AD is a progressive condition characterised by a gradual decline in cognitive and behavioral functions, including memory, language, executive function, and learning. Symptoms typically manifest after the age of 60, although early-onset cases have been observed in individuals in their 40 s and 50 s [2]. The disease generally follows a slow and steady progression, starting with mild cognitive impairments that often go unnoticed, eventually leading to significant memory loss and a loss of functional independence [3, 4]. Detecting AD in its early stages is crucial for clinical management, as available interventions—whether medical or behavioral—are most effective before extensive neuronal damage occurs. Although a cure has not yet been identified, current treatments focus on slowing disease progression [5, 6].

Structural magnetic resonance imaging (MRI) has become the gold standard in clinical practice for visualising disease-related brain changes, such as hippocampal atrophy and cortical thinning, due to its superior spatial resolution, excellent soft tissue contrast, and reduced health risks compared with computed tomography (CT) and positron emission tomography (PET) [7, 8] . Despite these advantages, AD presents unique computational challenges due to the morphological similarities observed in the early stages [9]. Advances in medical image analysis have significantly accelerated the development of computer-aided diagnostic systems [10]. However, translating high-resolution neuroimaging data into reliable diagnostic categories remains a formidable technical challenge. Traditional methods often struggle with the complexity and volume of brain data, requiring sophisticated computational frameworks to extract meaningful patterns. Deep learning models,

particularly convolutional neural networks (CNNs), have shown strong performance in extracting spatial features from neuroimaging data. However, their generalizability is often limited by issues such as class imbalance, and overfitting on small datasets [11, 12]. To address such fundamental limitations within medical image analysis, hybrid quantum-classical models have gained attention as a viable alternative approach. These models deliver richer, more expressive feature representations through the application of quantum principles, including superposition, entanglement, and interference [13, 14]. Quantum-classical approaches strengthen pattern recognition capabilities, especially within neuroimaging contexts, by facilitating quantum state manipulation that work alongside classical systems. The integration of quantum modules with classical neural networks enables the detection of subtle anatomical variations, especially those that signal early neurodegenerative changes. Quantum circuits exploit quantum state superposition to encode classical features within high-dimensional spaces.

The urgent need for reliable early detection of Alzheimer's disease (AD), particularly in the subtle transition from mild cognitive impairment to early dementia, calls for advanced computational solutions capable of identifying structural alterations before irreversible neuronal damage sets in. In response, this study introduces HQC-Net, a novel hybrid quantum-classical architecture specifically designed for four-class AD classification via structural MRI. The framework integrates classical feature extractors with variational quantum circuits, utilising multi-axis encoding and quantum Fourier transform (QFT) to detect spectral signatures associated with neurodegenerative progression. This work makes a significant contribution to the convergence of quantum computing and medical imaging by presenting a clinically relevant and technically robust model that addresses both theoretical and practical challenges in early-stage dementia diagnosis. The key contributions of this study are summarised as follows:

- A hybrid architecture is developed that integrates classical spatial encoders with variational quantum circuits for multiclass AD classification. This architecture features dynamic feature bifurcation, preserving both global contextual information and quantum-compatible representations.
- QFT and layered entanglement are employed to enhance feature representation, enabling the detection of global periodic patterns in cortical structures that characterise neurodegeneration processes—patterns that are often invisible to classical spatial analysis methods.
- Quantum noise simulation and error mitigation techniques are implemented to improve robustness under realistic hardware constraints. This includes detailed modelling of Noisy Intermediate-Scale Quantum (NISQ) devices, utilising mixed quantum channels and Richardson extrapolation for validation of practical deployment.
- A multihead attention mechanism is employed to fuse classical and quantum features into a unified decision space. This mechanism allows for the adaptive weighting of complementary quantum-classical strengths, tailored to the individual characteristics of each sample and the specific diagnostic requirements.

The remainder of this paper is structured to provide thorough coverage of the proposed methodology and its validation. Section 2 presents related works and current limitations in quantum-enhanced approaches to Alzheimer's disease classification. Section 3 details the proposed HQC-Net methodology, including datasets and preprocessing, classical feature extraction modules, quantum processing circuits, adaptive fusion mechanisms, and performance evaluation metrics. Section 4 presents detailed experimental results and a comparative analysis with state-of-the-art approaches, emphasising quantum circuit design innovations and their clinical implications. Finally, Section 5 concludes the study and outlines future research directions, establishing the foundation for quantum-enhanced medical imaging applications in clinical practice.

2. RELATED WORKS

Recent advancements in deep learning and machine learning have demonstrated significant potential across diverse medical imaging applications. These successes motivate continued exploration of deep learning frameworks for specialized tasks such as high-fidelity data unlearning [15-17]. In recent years, interest in hybrid quantum-classical machine learning models for brain disorder classification by neuroimaging data has increased. These approaches aim to overcome the limitations of conventional deep learning methods, particularly in tasks involving Alzheimer's disease (AD) diagnosis and staging. Early efforts focused on binary AD classification via structural MRI. In [18-20], variational quantum circuits were integrated with classical convolutional neural networks (CNNs), such as ResNet34 and AlexNet. Spatial features were extracted from T1-weighted axial or coronal MR images and mapped into quantum states via angle encoding schemes. These hybrid models, which were evaluated on simulated quantum back ends, achieved classification accuracies ranging from 95% to 97% on two-class datasets. However, their reliance on binary classification limits their clinical applicability, as AD progression involves multiple intermediate stages that require precise differentiation for effective treatment planning.

A more advanced architecture was proposed in [21], which combines vision transformers with variational quantum circuits embedded within multihead attention layers. Trained on the Kaggle and OASIS datasets, the model addresses class imbalance and interstage similarities by integrating entanglement-based quantum layers. While promising in managing class imbalance, the use of fixed quantum circuit templates limits the model's ability to capture the full morphological complexity of AD stages, particularly the subtle differences between mild cognitive impairment and early dementia. Multimodal neuroimaging approaches have also been explored. In [22], CNN and principal component analysis (PCA) were used to

extract MRI features, which were then encoded into quantum states for classification via a quantum support vector machine. The model leverages quantum kernels and entangled mappings to improve stagewise differentiation. However, reliance on PCA may have discarded essential spatial details required for accurate multiclass discrimination. Functional imaging has also been investigated. In [23], a hybrid quantum-classical CNN was applied to resting-state fMRI time series to detect early cognitive impairment on the basis of temporal brain dynamics. Similarly, [24] introduced a quantum-inspired model using EEG signals and a Goldner–Harary graph-based representation. Frequency-domain features from EEG were used to distinguish AD patients from healthy controls. While these functional approaches provide valuable complementary information, they require specialised acquisition protocols and extended scanning durations, limiting their practical integration compared with structural MRI.

Despite these new developments, however, several key limitations continue to constrain current quantum-enhanced AD classification approaches. First, most studies remain confined to binary or, at best, three-class classification tasks, ignoring the clinically relevant four-class staging needed for accurate disease assessment. Second, idealised quantum simulators disregard practical hardware limitations, such as quantum noise effects, decoherence, and substandard gate fidelity, which, on a large scale, considerably impact performance in realistic settings. Third, the bulk of existing architectures implement static quantum circuit layouts that do not exhibit adaptability to dataset variability and class imbalance. Finally, the integration of classical and quantum modules tends to oversimplify, restricting the synergy between hybrid systems. These drawbacks thus create space, therefore, for more adaptive and resilient quantum-classical models that can scale to handle complicated multiclass classification tasks while still being within the limitations enabled by near-term quantum hardware—an aim targeted by this current work.

3. THE PROPOSED METHODOLOGY

This work introduces HQC-Net, a neural architecture that seamlessly integrates classical and quantum components for multiclass medical image classification. The proposed framework overcomes the key limitations of conventional deep learning techniques by incorporating quantum-enhanced feature transformation and dynamic fusion strategies between quantum and classical representations. The architecture consists of four integrated components: (1) a hierarchical module for classical feature extraction, (2) a variational quantum circuit for quantum-level encoding, (3) a fusion module that adaptively integrates quantum and classical features, and (4) a multiclass classifier capable of distinguishing subtle diagnostic categories. The design leverages quantum phenomena such as superposition and entanglement while ensuring compatibility with the operational constraints of contemporary NISQ devices. An overview of the proposed HQC-Net architecture is presented in Figure. 1.

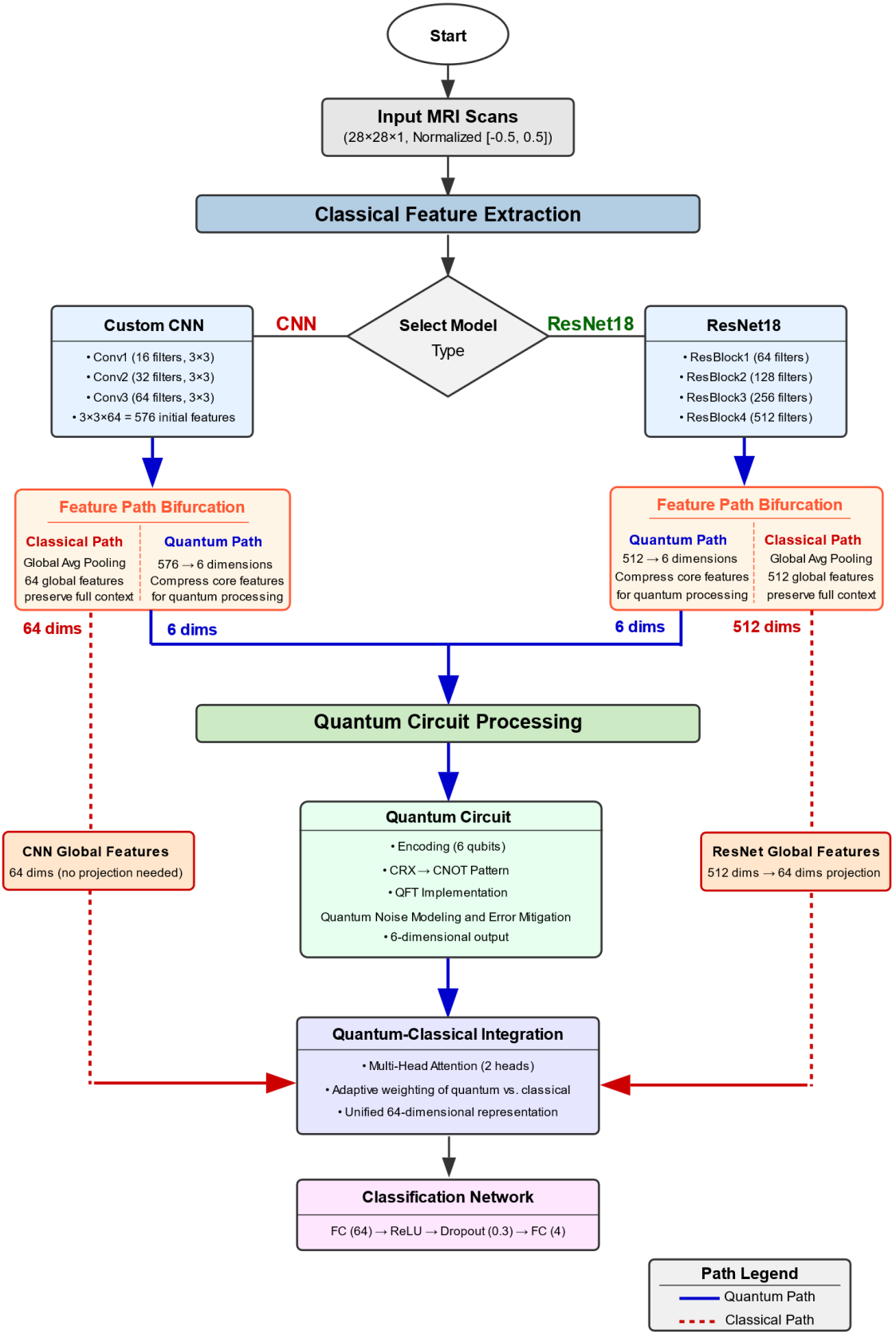

Fig. 1. The proposed model steps

3.1 AD Datasets

This study utilises two publicly available structural MR datasets: the Kaggle Alzheimer's MRI 4-class dataset and the Open Access Series of Imaging Studies (OASIS) dataset. These datasets provide complementary anatomical views—coronal slices in Kaggle and axial slices in OASIS—across four diagnostic stages of Alzheimer's disease (AD): nondemented (ND), very mild dementia (VND), mild dementia (MD), and moderate dementia (MOD). The combined use of these views enhances the coverage of key neuropathological features, including hippocampal atrophy and cortical thinning. Fig. 2 shows the class distributions within the Kaggle and OASIS datasets, both of which highlight the imbalance in sample counts across the four diagnostic stages. Fig. 3 presents representative MR slices selected from each class and dataset, demonstrating the anatomical features captured through the coronal and axial views, respectively. These figures collectively reflect the diversity, structure, and clinical complexity embedded in the datasets used for training and evaluation.

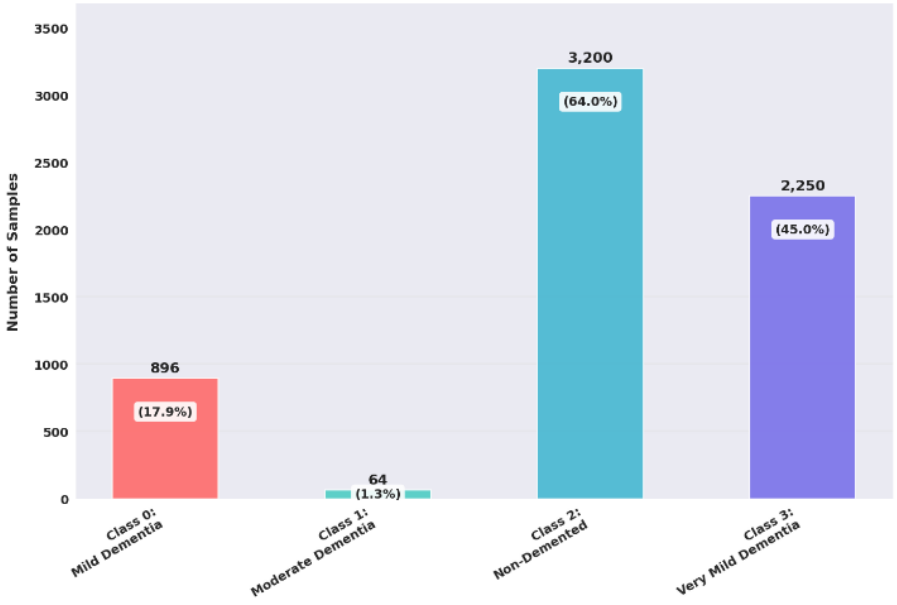

(A)

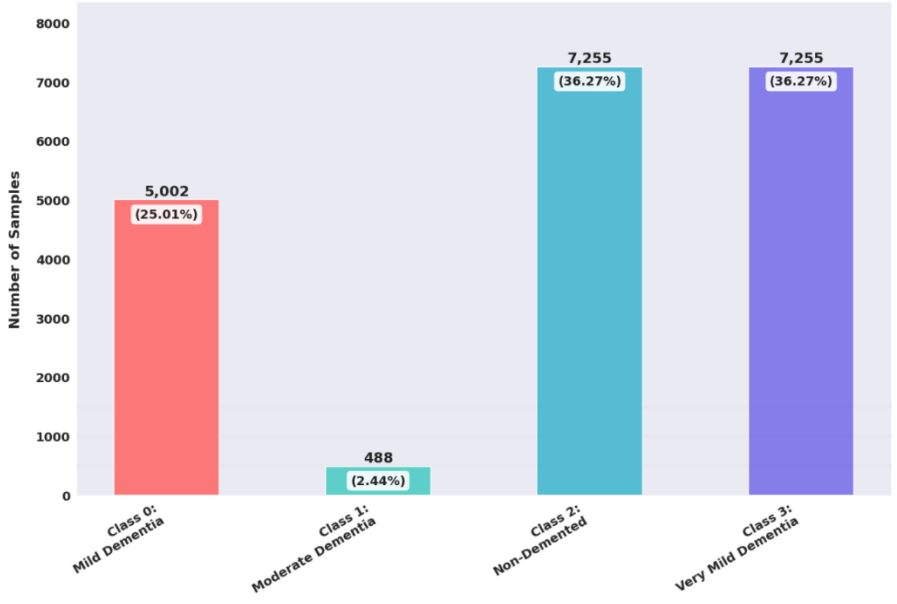

(B)

Fig. 2. Class distribution in the (A) Kaggle dataset and (B) OASIS dataset.

Both datasets are publicly accessible online. The Kaggle dataset is available at Alzheimer MRI 4 classes dataset, whereas the OASIS dataset can be accessed at OASIS Alzheimer's Detection .

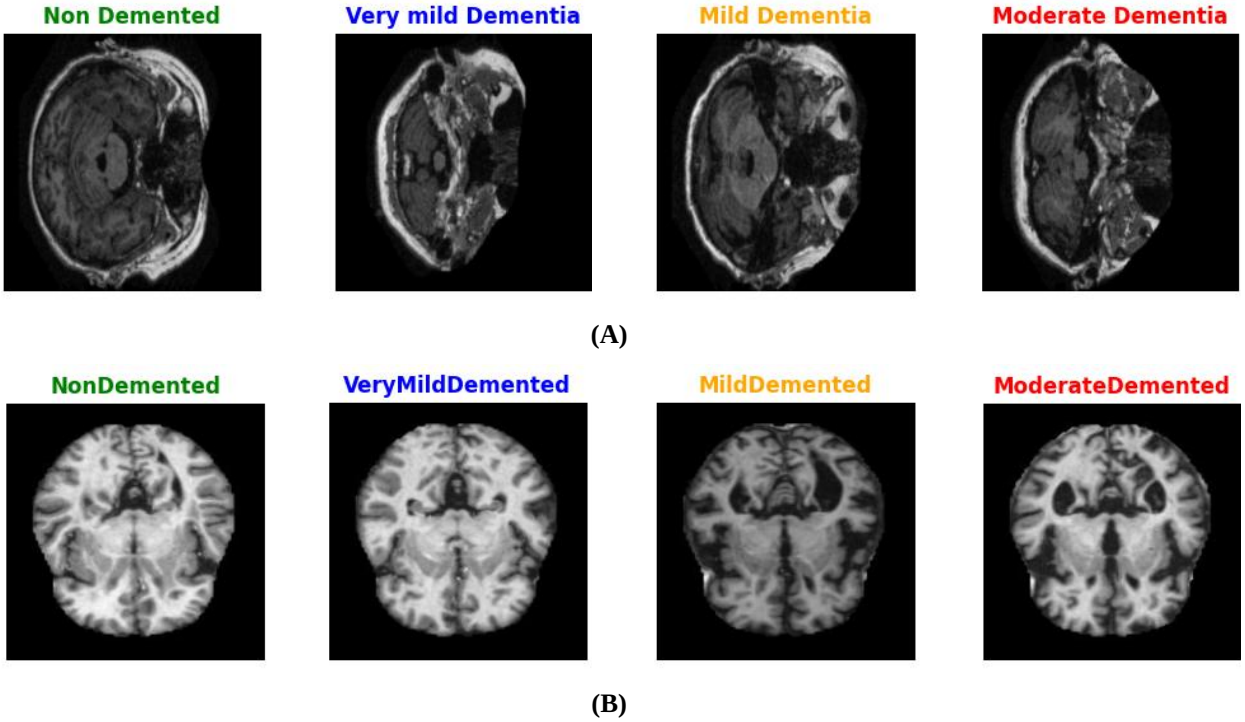

Fig. 3. Representative MRI scans showing: (A) Coronal slices from the Kaggle dataset, and (B) Axial slices from the OASIS dataset.

3.2 The Preprocessing Steps

To ensure optimal performance and training efficiency, a comprehensive preprocessing pipeline was implemented for the MR images prior to model input. Given the substantial processing overhead of quantum circuit operations—including multiaxis state encoding, entanglement generation, and QFT decomposition—this study deliberately adopted a lightweight preprocessing strategy to achieve a balance between quantum and classical components while maintaining diagnostic accuracy. Images were standardised to 28×28 pixel dimensions to balance efficiency with preservation of critical structural features essential for Alzheimer's disease classification. This approach avoided the burden of complex augmentation techniques that would compound the already intensive quantum processing requirements.

Pixel intensity normalisation was applied using a mean of 0.5 and standard deviation of 0.5, scaling values to the [-1, 1] range to enhance training stability and convergence behaviour. Advanced data loading optimisation was implemented through persistent worker allocation (n=2) and memory pinning strategies, effectively eliminating I/O bottlenecks while maintaining the optimal CPU-GPU resource distribution. Dataset partitioning followed an 80/20 training-validation protocol, allocating 16,000 training and 4,000 validation samples for OASIS and 5,131 training samples with 1,279 validation samples for Kaggle. This systematic preprocessing framework established a robust foundation for efficient model training and reliable performance evaluation.

3.3 The Classical Feature Extraction Stage

While CNNs effectively extract hierarchical spatial features in medical imaging, their performance in neuroimaging is often limited by dataset scarcity and class imbalance [25, 26]. To address these challenges, two separate backbone architectures are evaluated: a custom CNN and a modified ResNet18 encoder. Both approaches leverage transfer learning principles to maximise feature representation capacity across different scales.

3.3.1 Custom CNN

The CNN backbone processes 28×28 grayscale inputs through three hierarchical tiers with progressive feature map expansion (16→32→64 channels). Each tier comprises 3×3 convolutional layers, batch normalisation for training stability, ReLU activation for nonlinearity, and max pooling for spatial downsampling. This hierarchical design captures multiscale

features from fine-grained textures to global morphological patterns. Following the final convolutional tier, the architecture implements feature bifurcation to create parallel streams. The classical pathway applies global average pooling across spatial dimensions, producing 64-dimensional feature vectors that preserve global contextual information. Simultaneously, the quantum pathway flattens the 3×3×64 feature tensor into 576 dimensions, subsequently applying linear projection to generate 6-dimensional quantum-compatible encodings optimised for qubit operations, as illustrated in Figure. 4.

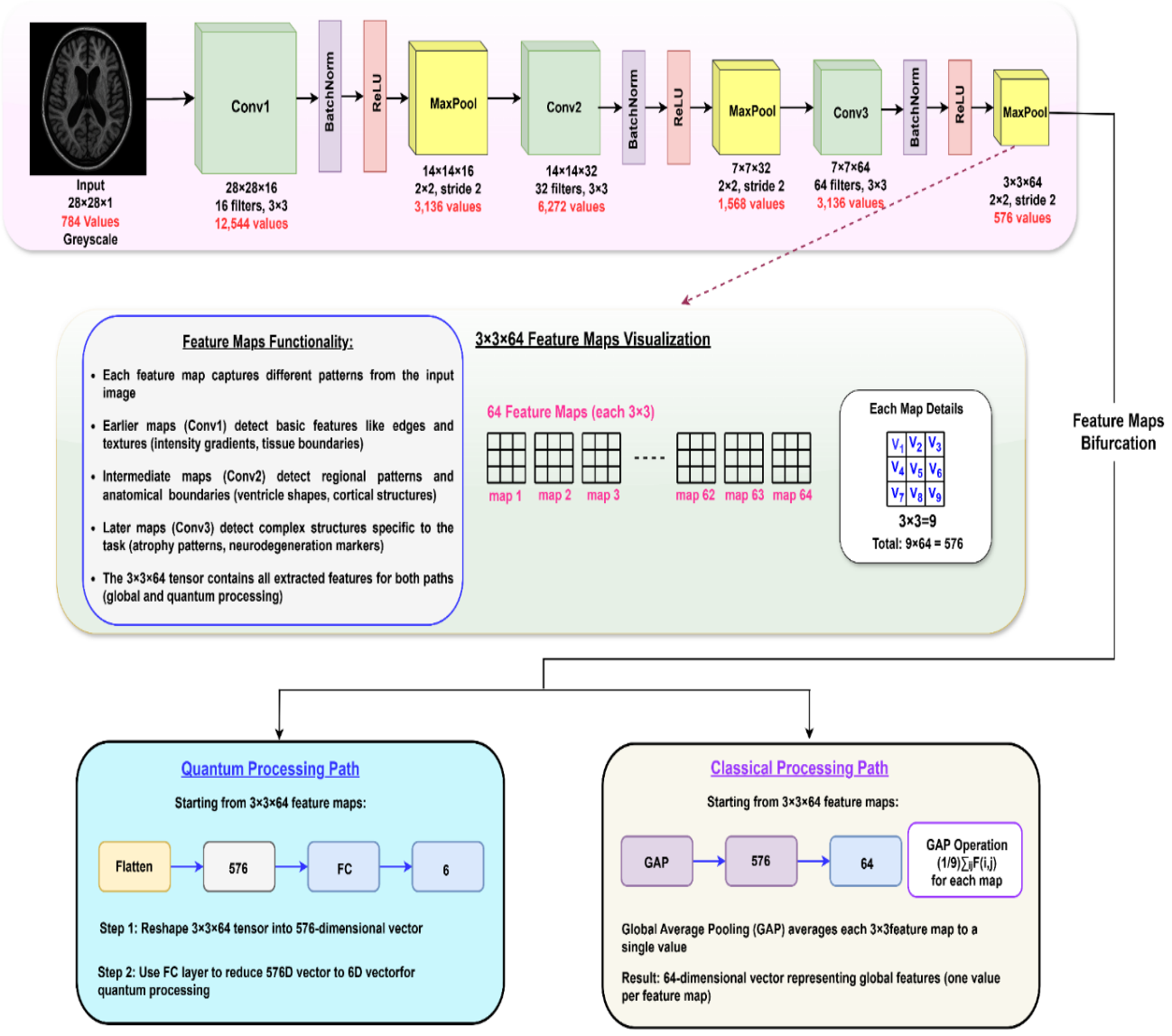

Fig. 4. Custom CNN Architecture for Feature Extraction

3.3.2 Modified ResNet18

The ResNet18 backbone incorporates residual learning principles specifically adapted for single-channel medical imaging. Key architectural modifications include single-channel input adaptation, a reduced initial kernel size (7×7→3×3) to preserve fine spatial details, and elimination of early max pooling to prevent information loss in small-scale inputs.

The network maintains four residual blocks with systematic channel expansion (64→128→256→512). Each block contains dual residual units with identity skip connections that facilitate gradient flow and feature preservation. Global average pooling transforms the final feature maps into 512-dimensional vectors, which undergo bifurcation into classical (512 dimensions) and quantum (6 dimensions via linear projection) pathways for subsequent operations, as depicted in Fig. 5.

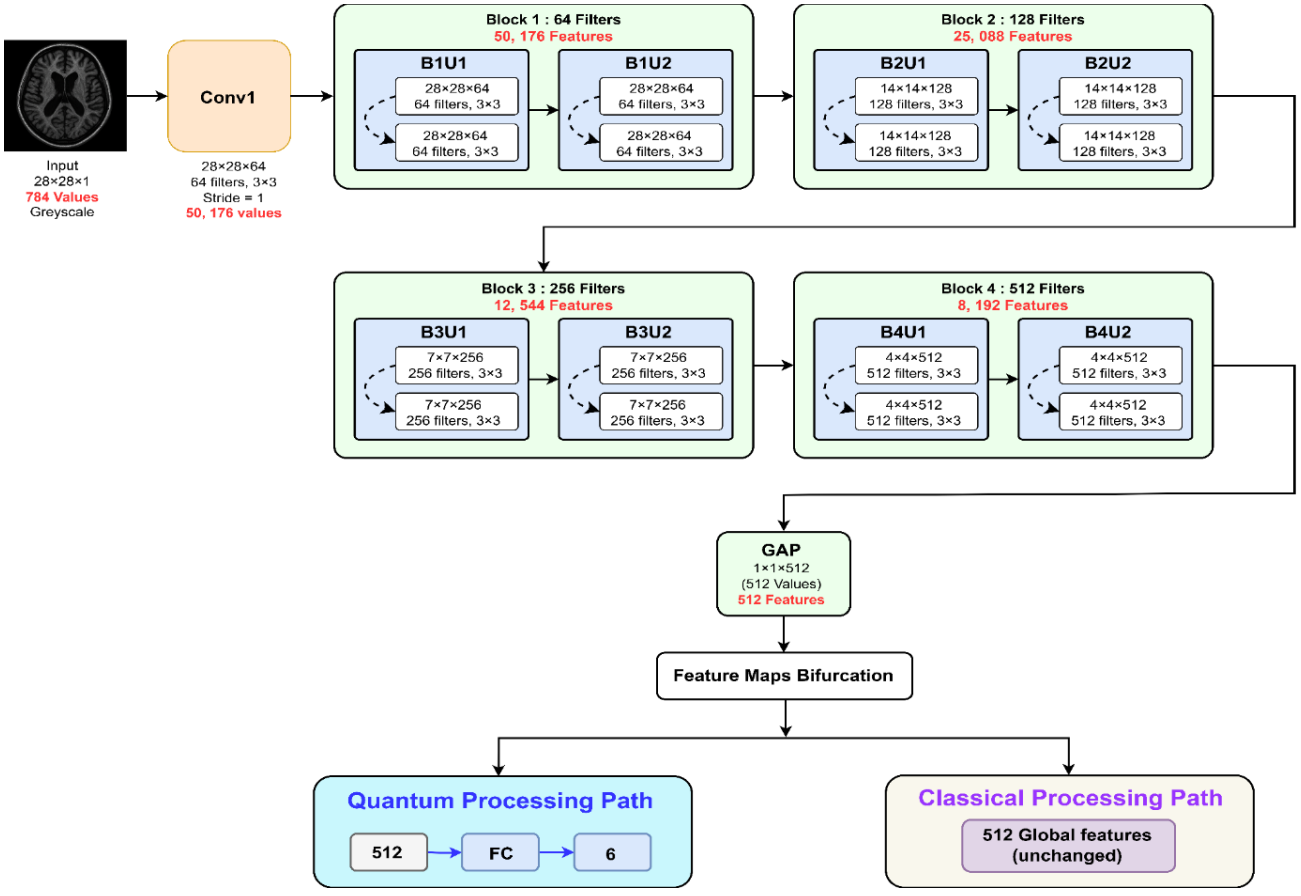

Fig. 5. Modified ResNet18 Architecture for Alzheimer's Classification

3.4 The feature selection stage using the quantum processing module

Quantum circuits exploit superposition and entanglement to process information in exponentially large state spaces [27], offering advantages for pattern recognition in high-dimensional medical data. The quantum module transforms classical features through a three-phase pipeline using 6 qubits. These phases include multiaxis rotation encoding, entanglement generation, and quantum Fourier transform processing to detect frequency-domain patterns that are not readily captured by spatial methods alone.

3.4.1 Variational Circuit

The quantum module, illustrated in Fig. 6, uses 6 qubits to capture complex feature interdependencies:

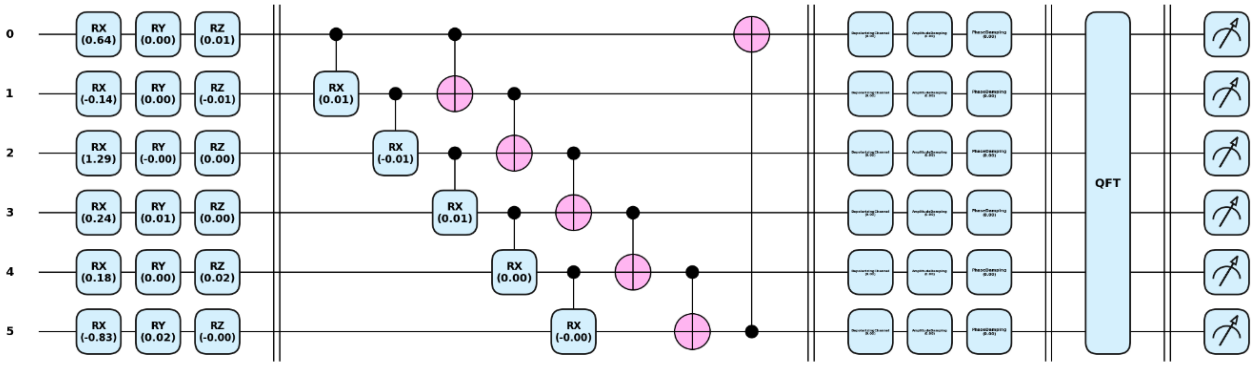

Fig. 6. Quantum Circuit Variants with Noise and QFT

State Preparation Phase: Multiaxis rotation encoding maps 6-dimensional classical features onto quantum states through consecutive RY, RZ, and RX operations for each qubit, where rotation angles directly correspond to normalised feature values.

Entanglement Generation Phase: Linear entanglement topology creates quantum correlations through nearest-neighbour CNOT gates connecting adjacent qubits sequentially (0→1, 1→2, 2→3, 3→4, 4→5). Parameterised controlled-RX gates applied to even qubit pairs enable adaptive quantum transformations that learn optimal feature relationships during training.

Frequency Domain Processing Phase: The quantum Fourier transform decomposes quantum states into frequency components [28-30], following a three-stage procedure: Hadamard gates for superposition, controlled-Rk rotations for phase relationships, and SWAP operations for qubit reordering. This approach enables frequency-domain analysis of cortical features, as shown in Fig. 7.

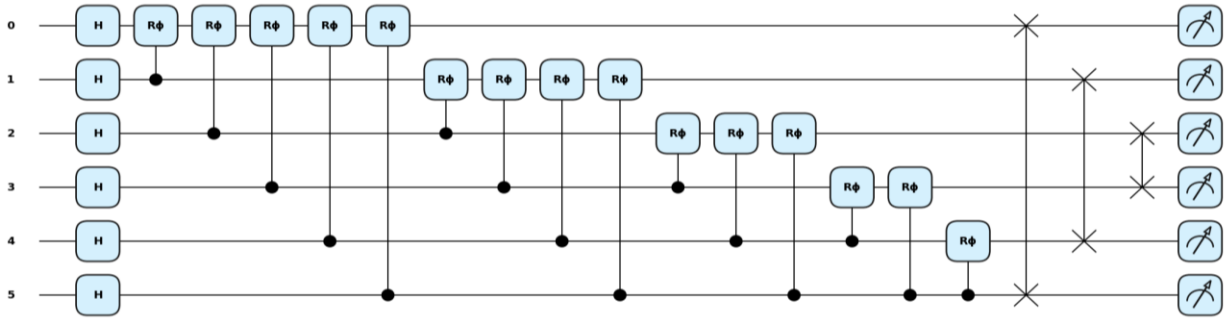

Fig. 7. Quantum Fourier Transform Implementation

3.4.2 Quantum noise modelling and error mitigation

To ensure NISQ device compatibility [31], the simulation incorporates realistic noise through mixed quantum channels: depolarising (probability of 0.01), amplitude damping (0.005), and phase damping (0.01). Richardson extrapolation across multiple noise levels [1.0, 1.5, 2.0] provides error mitigation by extrapolating toward noise-free performance.

3.5 Adaptive Fusion Module

Attention mechanisms enable dynamic feature weighting in multimodal systems [32], which is particularly critical for integrating heterogeneous quantum-classical representations. Multihead attention is employed to harmonise 6-dimensional quantum measurements with classical features (64/512 dimensions), projecting them into a unified 64-dimensional decision space.

Feature alignment between quantum and classical modalities occurs through trainable linear layers that map the inputs into a shared embedding space. A dual-head attention mechanism is applied, with each head processing a separate 32-dimensional subspace of the unified space, enabling the model to learn complementary feature relationships in parallel. Each attention head computes relevance scores across modalities and applies learned weight matrices to modulate feature contributions.

The outputs of both heads are concatenated and passed through a linear projection layer, producing a final fused 64-dimensional representation that captures integrated multimodal information. This design extends established attention principles in deep learning while addressing the unique challenges of hybrid quantum-classic medical image analysis.

3.6 Classification and Optimisation Framework

The final classification stage uses a two-layer network with specialised training strategies for quantum-classical parameter optimisation.

3.6.1 Classification Network

The classification network implements a two-stage architecture with hidden layer transformation (64→64 dimensions) via ReLU activation and dropout regularisation (probability of 0.3), followed by multinomial classification (64→4 dimensions) with softmax normalisation for multiclass categorisation, as outlined in Figure. 8.

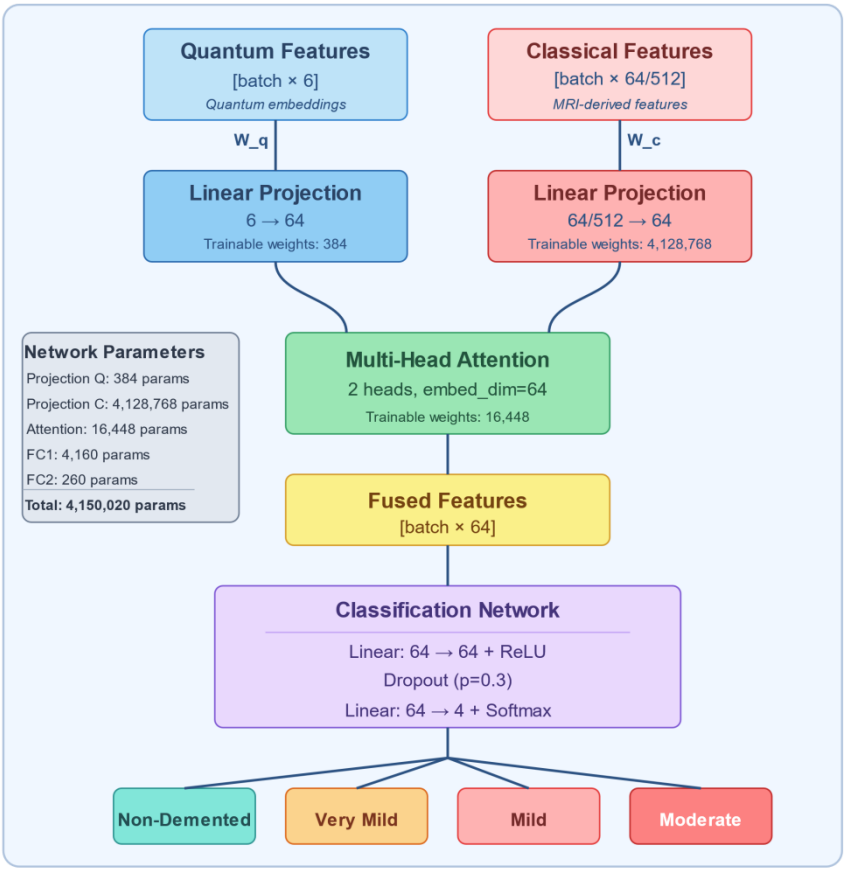

Fig. 8. Feature Fusion to the Classification Pipeline

3.6.2 Training strategy

Training employs the Adam optimiser with adaptive learning rate scheduling (initial learning rate 1×10^{-3}, reduction factor 0.5, patience 3 epochs). Gradient clipping (threshold of 1.0) ensures stable quantum parameter updates, whereas selective L2 regularisation ($\lambda = 1 \times 10^{-4}$) applies exclusively to classical parameters. The exponential moving average (decay factor $\alpha = 0.999$) provides temporal smoothing across heterogeneous parameter spaces, addressing the distinct optimisation characteristics of quantum and classical components. All the hyperparameters used in the proposed methodology are organised in Table I.

TABLE I. TRAINING HYPERPARAMETERS AND CONFIGURATION

Parameter	Value	Description
Optimiser	Adam	Adaptive learning rate optimisation
Initial Learning Rate	1×10^{-3}	Starting learning rate for all parameters
Learning Rate Scheduler	ReduceLROnPlateau	Reduction factor: 0.5, patience: 3 epochs
Batch Size	32	Training and validation batch size
Maximum Epochs	50	Training termination criterion
Dropout Rate	0.3	Regularisation in classification layer
L2 Regularisation	1×10^{-4}	Applied exclusively to classical parameters
Gradient Clipping	1.0	Threshold for quantum parameter stability
EMA Decay Factor	0.999	Exponential moving average for smoothing
Input Resolution	28×28 pixels	Standardised image dimensions
Normalisation Range	[-1, 1]	Pixel intensity scaling
Data Workers	2	Persistent workers with memory pinning
Quantum Qubits	6	Circuit register size
QFT Implementation	Full 6-qubit	Hadamard + Controlled-R + SWAP gates
Noise Simulation	Mixed channels	Depolarising: 0.01, Amplitude: 0.005, Phase: 0.01
Error Mitigation	Richardson Extrapolation	Scaling factors: [1.0, 1.5, 2.0]
Reset Probability	0.1	Error accumulation prevention

Algorithm 1 provides a comprehensive overview of the complete HQC-Net framework, detailing the systematic integration of classical feature extraction, quantum processing, attention-based fusion, and optimisation strategies described throughout the methodology section.

Algorithm 1 HQC-Net: Hybrid Quantum-Classical Alzheimer's Classification

Require: Kaggle (5,121), OASIS (20,000) MRI datasets where $x_i \in \mathbb{R}^{28\times28}$, $y_i \in \{0, 1, 2, 3\}$ (Non-Demented, Very Mild, Mild, Moderate)
Ensure: Trained QCNN and QResNet18 models

Phase 1: Data Preprocessing:
Resize images to 28×28, normalise to $[-1, 1]$;
Split datasets: **80% train, 20% validation**;

Phase 2: Model Initialisation:
for Architecture $\mathcal{A} \in \{QCNN, QResNet18\}$ **do**
    Initialise classical backbone for $\mathcal{A}$;
    Setup 6-qubit quantum circuit with trainable parameters;
    Initialise Multi-Head Attention (2 heads, 64-dim);
    Setup classifier network (64→64→4);
    Configure Adam optimiser ($\alpha = 10^{-3}$);
end for

Phase 3: Hybrid Training Loop:
for each model and epoch $e = 1$ to 50 **do**
    for each batch (x, y) where $y \in \{0, 1, 2, 3\}$ (Non-Demented, Very Mild, Mild, Moderate) **do**
        Classical Feature Extraction:
        $f_c = \text{Backbone}(x)$;
        $f_q = \tanh(W_q f_c + b_q)$ where $f_q \in \mathbb{R}^6$;
        Quantum Processing:
        Initialise: $|\psi\rangle = |000000\rangle$;
        Apply multi-axis rotations: R_Y, R_Z, R_X for each qubit;
        Apply entanglement: CNOT chain + CRX gates;
        Apply Quantum Fourier Transform;
        Apply NISQ noise and measure: $F_q^{out} = \langle Z_i \rangle$;
        Fusion and Classification:
        Project features to common space: $\tilde{f}_c, \tilde{f}_q \in \mathbb{R}^{64}$;
        $I_{fused} = \text{MultiHeadAttention}([\tilde{f}_c, \tilde{f}_q])$;
        $\text{logits} = \text{Classifier}(I_{fused})$;
        Optimisation:
        $\mathcal{L} = \text{CrossEntropy} + \text{L2-regularisation}$;
        Update parameters with gradient clipping;
    end for
    Validate and apply learning rate scheduling;
end for

Phase 4: Error Mitigation:
Apply Richardson extrapolation with noise scales [1.0, 1.5, 2.0];
Extrapolate to zero-noise performance;

Phase 5: Evaluation:
Compute comprehensive metrics: accuracy, precision, recall, F1, AUC;
Generate confusion matrices and ROC curves;

Return:
QCNN: 95.71% (Kaggle), 99.58% (OASIS)
QResNet18: 97.56% (Kaggle), 99.67% (OASIS)

3.7 Performance evaluation

The evaluation employs multiple complementary metrics to provide a comprehensive assessment of classification performance across the four Alzheimer's disease stages:

1. Overall accuracy: The overall accuracy is the proportion of correctly classified samples across all classes, providing a global performance indicator.

2. Per-class accuracy: The classification accuracy for each individual disease stage, enabling the detection of potential biases in model performance across diagnostic categories.

3. Confusion matrix: A detailed breakdown of predictions versus ground truth, revealing specific misclassification patterns that may have clinical significance. This includes an analysis of whether errors occur between adjacent disease stages or across disparate categories.

4. Precision, Recall, and F1-Score: Class-specific metrics that provide complementary perspectives on model performance, particularly valuable for imbalanced diagnostic categories:

- Precision $= \frac{TP}{TP+FP}$ - Indicates the reliability of positive predictions

- Recall $= \frac{TP}{TP+FN}$ - Indicates the ability to detect all positive cases.

- F1-Score $= 2 \times \frac{\text{Precision} \times \text{Recall}}{\text{Precision} + \text{Recall}}$ - Harmonic mean of precision and recall.

5. ROC curves and AUC: Receiver operating characteristic curves and the corresponding area under the curve values for each class, including the macroaverage AUC, offering threshold-independent performance assessment.

6. Precision-Recall Curves and Average Precision: This metric is particularly informative for imbalanced medical datasets where minority classes often represent critical diagnostic categories.

These metrics are computed on the validation set, which serves as the test set to ensure unbiased performance estimation. Figure. 9 illustrates the confusion matrix for Alzheimer's disease classification.

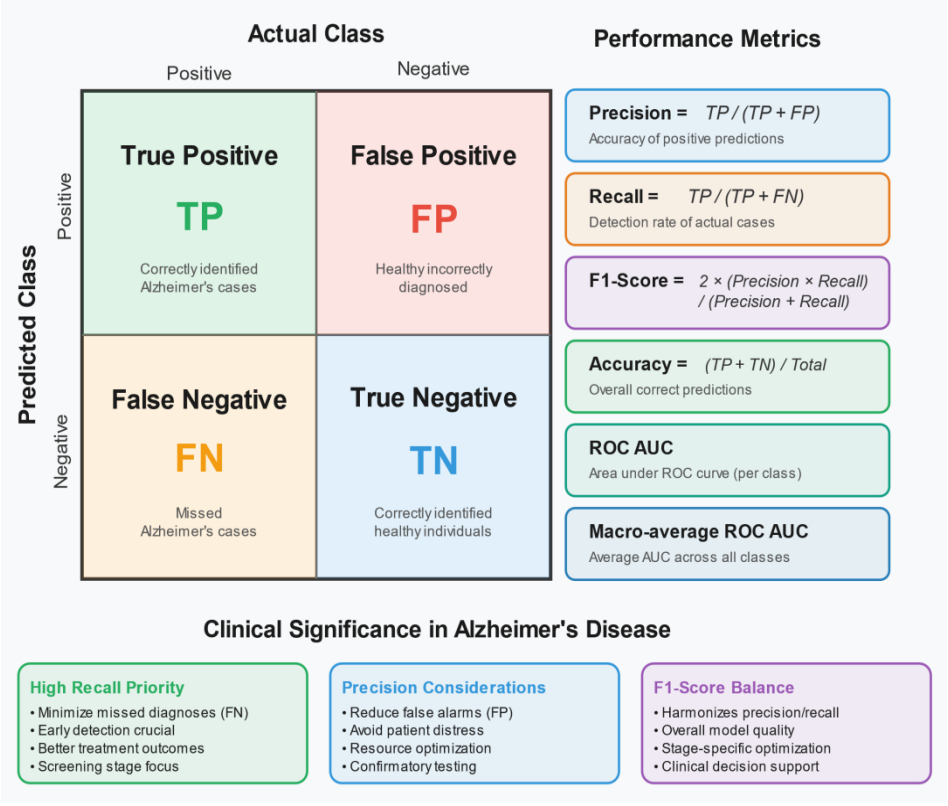

Fig. 9. Confusion Matrix for Alzheimer's Disease Classification

4. RESULTS AND DISCUSSION

This section presents a comprehensive evaluation of our proposed hybrid quantum-classical architectures across two neuroimaging datasets, emphasising quantum circuit design innovations and their clinical implications for multiclass Alzheimer's disease classification. All the experiments were conducted via Google Colab Pro with NVIDIA Tesla V100 GPUs, and the quantum simulations were performed via PennyLane's default mixed device with realistic noise modelling.

4.1 Performance Comparison across Architectures

Table II presents the performance results for all the experimental configurations, revealing important patterns in hybrid model behaviour.

TABLE II. COMPLETE PERFORMANCE RESULTS OF THE PROPOSED HYBRID ARCHITECTURES

Architecture	Dataset	Test Accuracy (%)	ROC AUC	Macro Avg F1	Weighted Avg F1	Training Time (hrs)
QCNN	Kaggle	95.71	0.9954	0.95	0.96	4.02
QCNN	OASIS	99.58	0.9997	1.00	1.00	14.90
QResNet18	Kaggle	97.56	0.9969	0.94	0.98	5.55
QResNet18	**OASIS**	**99.67**	**1.0000**	**1.00**	**1.00**	**13.18**

The results demonstrate substantial variation in performance across different model–dataset combinations. On the Kaggle dataset, the modified QResNet18 achieves superior accuracy (97.56%) compared with the custom QCNN (95.71%), reflecting the benefits of deeper feature extraction. However, both models show reduced performance on this smaller, more imbalanced dataset compared with the OASIS results.

The OASIS dataset yields exceptional performance across both architectures. The custom QCNN achieves 99.58% test accuracy with a near-perfect AUC (0.9997), whereas the modified QResNet18 achieves the highest overall performance, with 99.67% accuracy and perfect discriminative capability (AUC = 1.0000). These results demonstrate the effectiveness of quantum-classical hybrid processing when sufficient training diversity is available.

The AUC values reveal excellent rank-ordering performance across all configurations, ranging from 0.9954--1.0000. The modified QResNet18's perfect AUC on OASIS indicates optimal separation between all four diagnostic categories, which is crucial for multiclass clinical applications. Even under challenging conditions such as severe class imbalance on Kaggle, quantum circuits maintain strong discriminative ability (AUC > 0.995).

Macroaverage F1 scores demonstrate balanced performance across diagnostic categories. The OASIS configurations achieve perfect macro F1 scores (1.00), indicating equal effectiveness across all disease stages. The Kaggle results show slightly lower macro F1 values (0.94--0.95) due to class imbalance effects, particularly the underrepresented moderate dementia category. The weighted F1 scores consistently match or exceed macro values, confirming robust overall classification performance.

4.2 Training dynamics and computational analysis

Training efficiency varies significantly across models and datasets, as shown in Table II. On the Kaggle dataset (5,121 samples), the custom QCNN trains fastest at 4.02 hours because its lightweight 3-layer architecture produces 64-dimensional features. The modified QResNet18 requires 5.55 hours, reflecting the computational overhead of its deeper backbone in generating 512-dimensional vectors.

For the OASIS dataset (20,000 samples), the training time increases substantially: the custom QCNN requires 14.90 hours, whereas the modified QResNet18 needs 13.18 hours. The larger dataset size and quantum circuit processing demands explain these extended training periods. Interestingly, modified QResNet18 trains slightly faster than does the QCNN on OASIS despite its deeper architecture, suggesting better optimisation efficiency with larger datasets.

The training behaviours illustrated in Fig. 10 demonstrate the distinct optimisation characteristics typical of quantum–classical hybrid systems. The custom QCNN model on the Kaggle dataset shows prominent oscillations within the validation accuracy between 40% and 95% over the first 20 epochs, as illustrated in Fig. 10a. These oscillations highlight the optimisation difficulties experienced while handling highly imbalanced datasets, particularly the fact that only 11 Moderate Dementia samples exist. The quantum circuit fails to converge to steady-state parameter settings for this underrepresented class, consequently resulting in extensive exploration of the parameter space governed by multiaxis rotational encoding (RY → RZ → RX). Convergence begins to stabilise around epoch 25, as the optimiser identifies parameter settings that facilitate consistent classification across all categories despite the inherent data imbalance.

In contrast, the QCNN trained on the OASIS dataset exhibits considerably smoother convergence across the 50 training epochs, as illustrated in Fig. 10b, with the validation accuracy progressively increasing from 60% to 99.38%. This stability

stems from the OASIS dataset's richer statistical properties and better class balance across diagnostic categories, enabling more consistent training behavior. The modified QResNet18 architecture shows better convergence patterns on both datasets, as demonstrated in Figure. 10c and Figure. 10d. This improvement results from its deeper classical backbone, which generates higher-quality feature representations and facilitates quantum parameter optimisation despite class imbalance challenges.

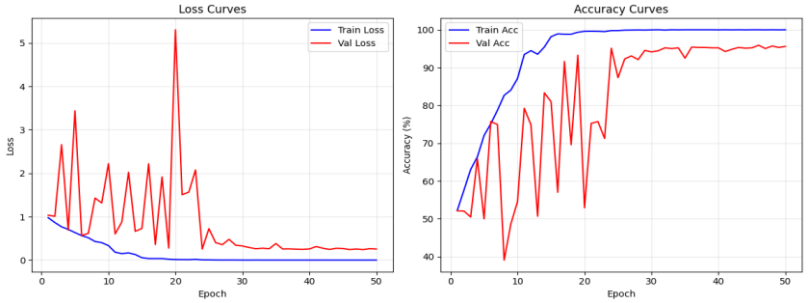

A

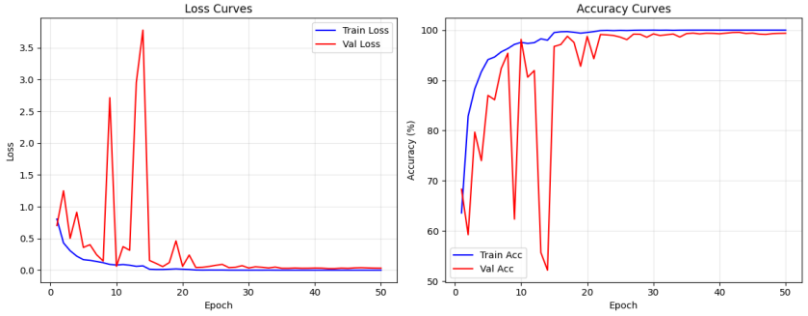

B

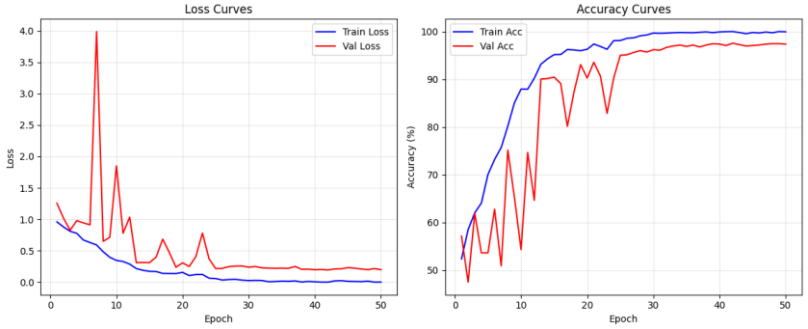

C

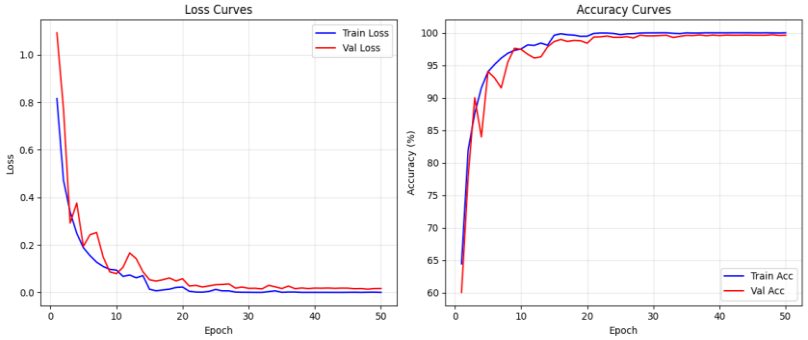

D

Fig. 10. Training Dynamics and Learning Curves (a) QCNN - Kaggle Dataset: (b) QCNN - OASIS Dataset (c) Modified QResNet18 - Kaggle Dataset: (d) Modified QResNet18 - OASIS Dataset.

4.3 Discriminative Performance Analysis

Table III reveals the differential effectiveness of quantum processing across Alzheimer's disease stages, demonstrating enhanced discrimination between morphologically similar categories. The performance variations highlight the impact of data availability on quantum circuit effectiveness. On Kaggle, the uniform 90.91% accuracy for moderate dementia across both architectures demonstrates the remarkable ability of quantum circuits to extract meaningful patterns from severely underrepresented classes. This performance validates the robustness of the quantum processing approach in handling natural class imbalances and supports the decision to avoid artificial data augmentation or class balancing techniques, allowing the model to learn from authentic clinical data distributions. In contrast, the OASIS results demonstrate the quantum processing potential when sufficient statistical diversity enables proper state formation, achieving perfect moderate dementia classification across all configurations.

TABLE III. PER-CLASS ACCURACY COMPARISON

Method/Dataset	Non-Demented	Moderate Dementia	Mild Dementia	Very Mild Dementia
QCNN - Kaggle	94.44%	90.91%	97.46%	93.87%
QCNN - OASIS	99.16%	100.00%	100.00%	99.65%
QResNet18 - Kaggle	95.14%	90.91%	98.44%	97.49%
QResNet18 - OASIS	99.23%	100.00%	100.00%	99.86%

Table IV displays the overall classification metric results for all stages and datasets, which exhibit clinically significant precision-vs-recall trade-offs. On the OASIS dataset, both hybrid models demonstrate a remarkable balance, with precision and recall consistently exceeding 0.99, indicating decision stability across all diagnostic stages. However, the Kaggle results demonstrate structural variation in addressing class imbalance and limited representation. The modified QResNet18 exhibits a discrepancy between precision and recall (precision 0.77, recall 0.91), indicating the impact of combining deeper classical feature extraction with quantum circuits. The custom QCNN exhibits optimal precision (1.00) and somewhat lower recall (0.91), demonstrating that its combined architecture enables more stable quantum states to be encoded and more conclusive predictions. These results demonstrate that while diversity improves performance, hybrid quantum-classical models maintain stability across diverse distributions. The ability of these methods to adapt to diverse dataset characteristics while achieving clinically significant performance confirms their suitability for practical application in neuroimaging.

TABLE IV. DETAILED CLASSIFICATION METRICS

Kaggle Dataset Performance					
Method	***Class***	***Precision***	***Recall***	***F1-Score***	***Support***
QCNN	Non-Demented	0.94	0.94	0.94	144
	Moderate Dementia	1.00	0.91	0.95	11
	Mild Dementia	0.97	0.97	0.97	512
	Very Mild Dementia	0.94	0.94	0.94	359
Modified QResNet18	Non-Demented	0.99	0.95	0.97	144
	Moderate Dementia	0.77	0.91	0.83	11
	Mild Dementia	0.98	0.98	0.98	512
	Very Mild Dementia	0.96	0.97	0.97	359
OASIS Dataset Performance					
Method	***Class***	***Precision***	***Recall***	***F1-Score***	***Support***
QCNN	Non-Demented	1.00	0.99	0.99	1429
	Moderate Dementia	1.00	1.00	1.00	90
	Mild Dementia	1.00	1.00	1.00	1046
	Very Mild Dementia	0.99	1.00	0.99	1435
Modified QResNet18	Non-Demented	1.00	0.99	1.00	1429
	Moderate Dementia	0.99	1.00	0.99	90
	Mild Dementia	1.00	1.00	1.00	1046
	Very Mild Dementia	1.00	1.00	1.00	1435

Figure. 11 shows visual evidence of discriminative performance via ROC and precision–recall (PR) curves across all experimental configurations. The curves exhibit steep and well-separated trajectories, indicating strong interclass discrimination. PR patterns further demonstrate consistent behaviour across varying decision thresholds, reinforcing the robustness of the hybrid architecture. Notably, both the ROC and PR curves retain high discriminative gradients even under severe class imbalance, supporting threshold-independent reliability—an essential feature for deployment in diverse clinical settings.

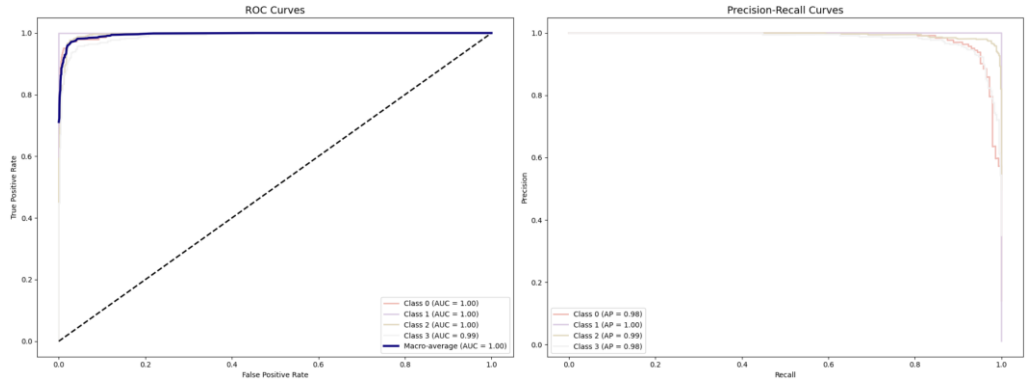

A

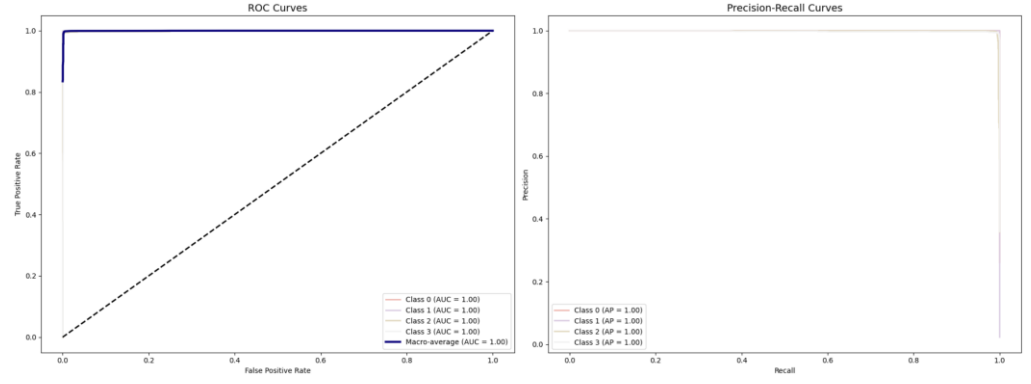

B

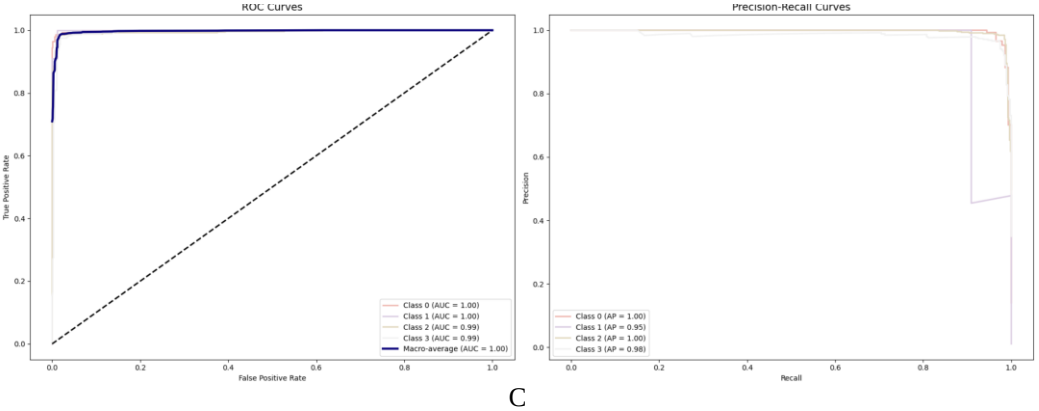

C

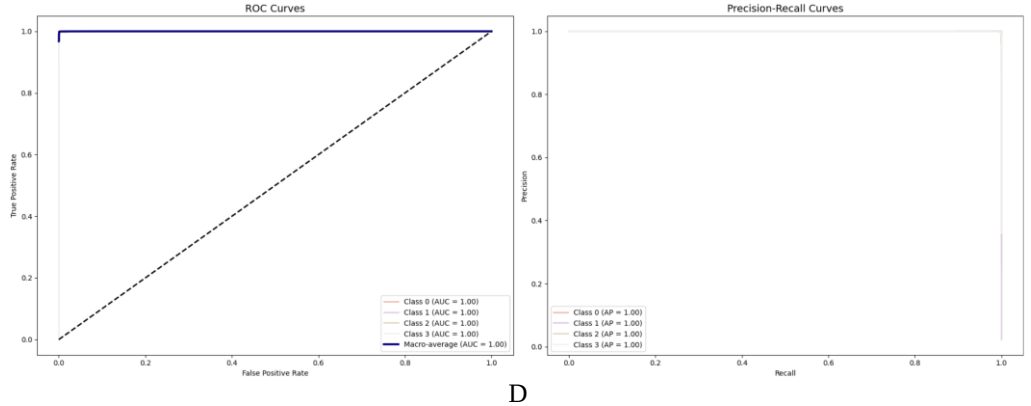

D

Fig. 11. ROC and Precision-Recall Analysis (a) QCNN - Kaggle (b) QCNN - OASIS (c) Modified QResNet18 - Kaggle (d) Modified QResNet18 - OASIS.

Figure. 12 provides detailed insight into misclassification patterns through confusion matrix analysis across all experimental configurations. The matrices reveal distinct error distributions between datasets, with OASIS configurations demonstrating superior classification accuracy, as evidenced by stronger diagonal concentration, whereas Kaggle matrices show increased off-diagonal elements reflecting the challenging data conditions. These visual patterns confirm the quantitative results presented in Tables II and IV, providing matrix-level validation of the performance differences observed across the experimental configurations.

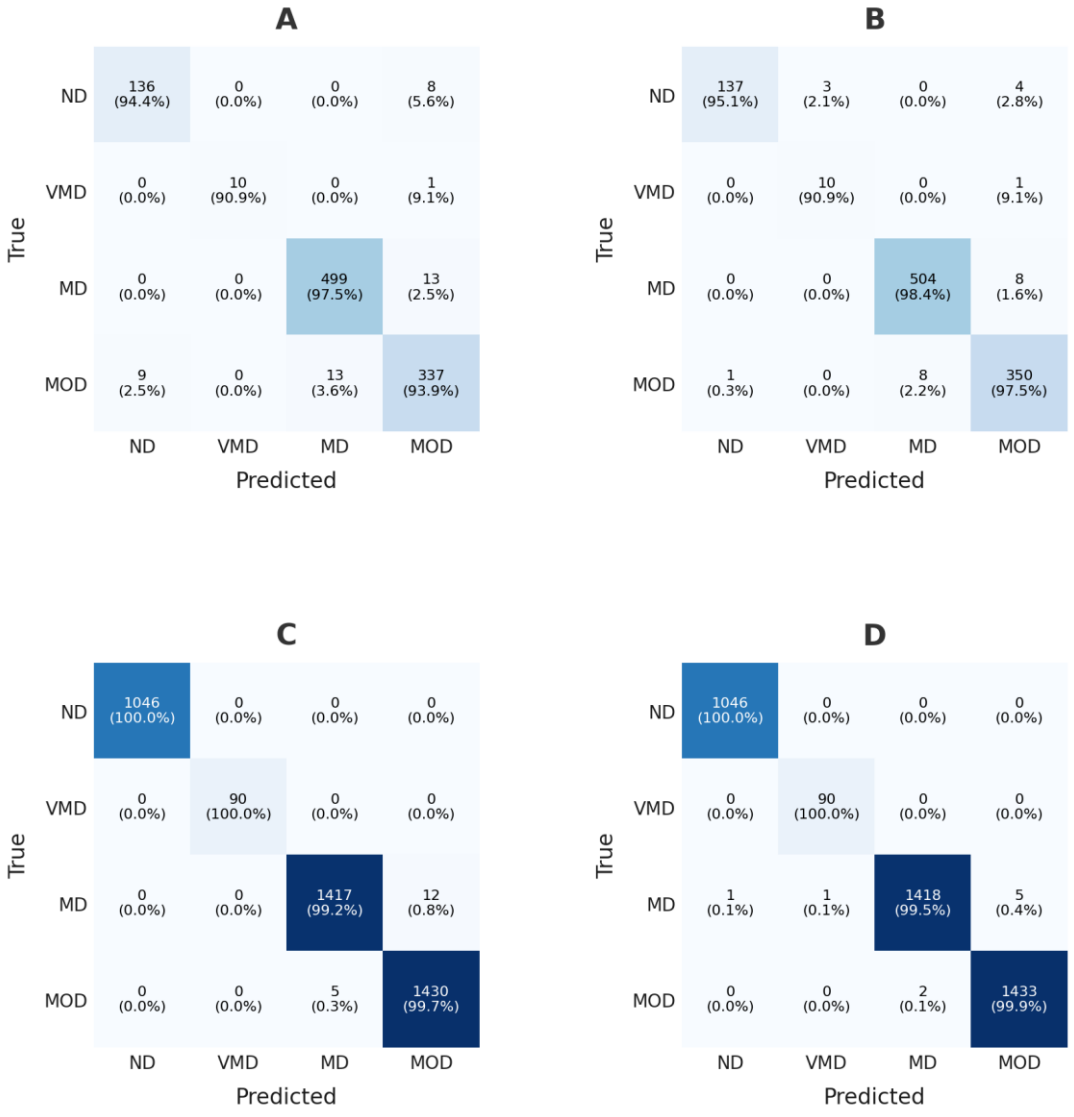

Fig. 12. Confusion matrices for classification analysis (a) QCNN – Kaggle (b) Modified QResNet18 - Kaggle (c) QCNN - OASIS (d) Modified QResNet18 - OASIS

Figure. 13 shows the classification accuracy across disease stages via class-specific bar charts. The visualisations provide clear visual evidence of performance consistency within each dataset, with OASIS configurations showing uniformly high accuracy bars across all diagnostic categories, whereas Kaggle configurations display greater height variation between disease stages.

Both hybrid architectures demonstrate measurable accuracy levels across the diagnostic spectrum, with Modified QResNet18 generally achieving higher bar heights than Custom QCNN on both datasets. The visual comparison between datasets reinforces the performance patterns observed throughout the experimental evaluation, providing graphical confirmation of the models' comparative effectiveness across different data conditions.

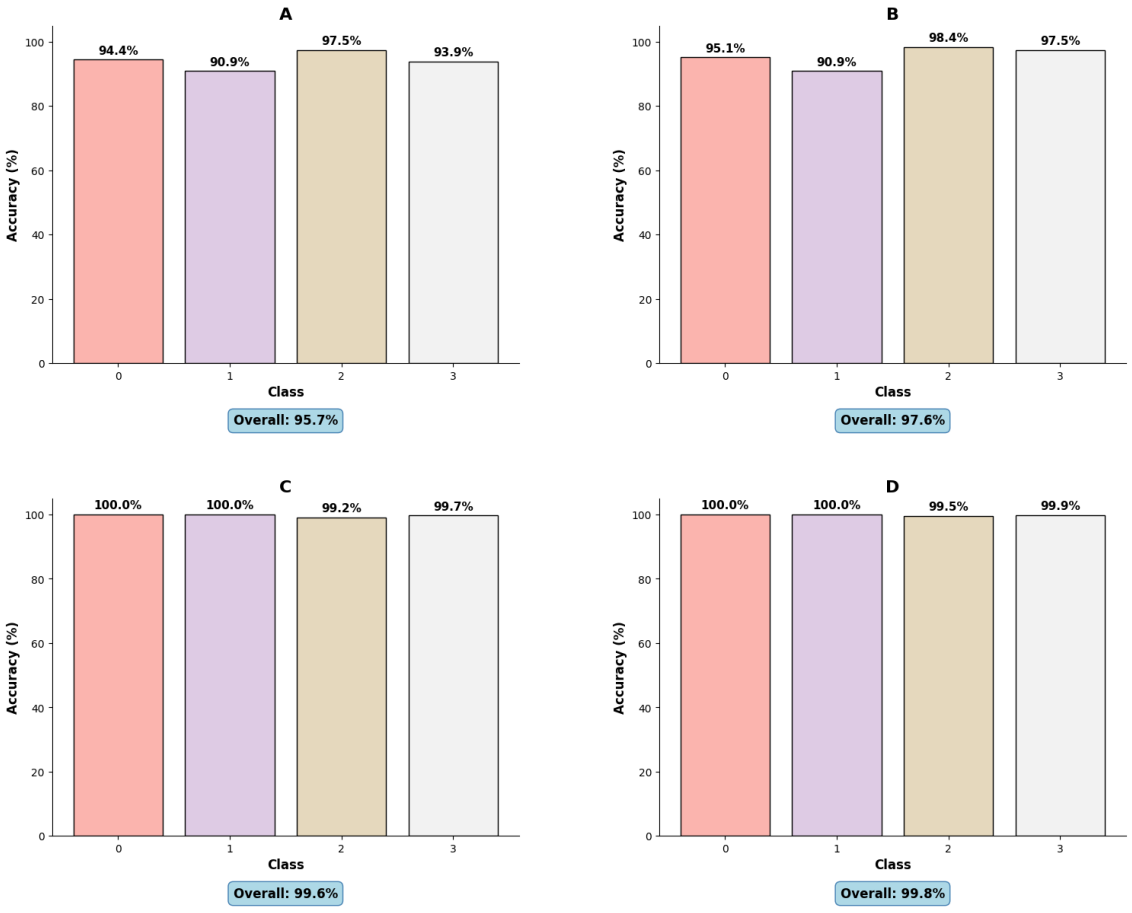

Fig. 13. Per-class accuracy visualisation (a) QCNN - Kaggle (b) QCNN - OASIS (c) Modified QResNet18 - Kaggle (d) Modified QResNet18 - OASIS

4.4 Quantum Processing Performance Analysis

The validation of the quantum processing illustrates specific computational benefits that warrant the hybrid method beyond mere performance metrics. The preservation of discriminative capability by the quantum circuit using sparse training samples provides an intrinsic advantage that quantum state superposition offers towards managing sparse clinical information—a typical problem in rare disease diagnoses where sample collection is inherently difficult.

The multiaxis rotation encoding is particularly valuable for registering complex morphological relationships that may become computationally expensive to represent explicitly via traditional methods. The state space of quantum states allows simultaneous encoding of multiple anatomical perspectives of anatomy and consequently recognition of faint correlations between features that improve diagnostic accuracy without requiring extensive classical feature engineering.

The QFT component provides computational speedup on typical frequency-domain analysis via classic Fourier methods, particularly when handling large medical image datasets. Such quantum processing among frequencies serves to detect predictive patterns of early neurodegeneration that exist among periodic brain structures—patterns that classic spatial analyses might require many additional computations to recognise consistently.

The confirmation of noise resilience confirms that quantum processing still has computational strengths within realistic hardware limitations, supporting the practical viability of quantum-enhanced medical imaging systems as quantum technology has developed further.

4.5 Feature Fusion and Multihead Attention Mechanisms

The consistently high performance achieved across a range of dataset characteristics and architectural conditions validates the effectiveness of the multihead attention fusion strategy employed by the hybrid model. The attention mechanism's ability to adaptively weight classical and quantum features emerges as a key rationale behind the identified robustness, which stands evident within the retention of strong performance by the model despite significant variations in data distribution and imaging perspectives.

The dual-head architecture's success in achieving balanced performance by diagnostic class manifests its capacity to manage the inherent challenge of incorporating heterogeneous features. Compared with fixed combination approaches that apply fixed combination rules, the learned attention weights obtain dynamic flexibility to adjust to the particular traits of each example, which explains the improved discriminative power evident from the experimental results. This adaptive capability is particularly valuable in clinical scenarios where the relative importance of spatial and frequency-domain features may vary with disease presentation and imaging conditions.

The attention-based combination mechanism additionally facilitates the computational efficiency of the model by focusing processing resources on the most diagnostically relevant feature combinations for each case. This targeted approach helps explain the maintained performance quality even when transitioning between different classical backbone architectures, as the attention mechanism can adapt to varying feature dimensionalities while preserving essential discriminative information.

Furthermore, the consistent performance across both the coronal and axial imaging orientations suggests that the attention mechanism successfully identifies and emphasises the most informative features regardless of the anatomical perspective. This orientation-independent effectiveness supports the practical deployment potential of the hybrid approach across diverse clinical imaging protocols and equipment configurations.

4.6 Comparative Analysis and Scientific Advancement

The experimental results position the proposed approach among the leading quantum-enhanced medical imaging methods. Table V shows that the modified QResNet18 achieves 99.67% accuracy on OASIS, substantially outperforming previous quantum-enhanced approaches: 15.37 percentage points over ViT-based methods [21] and 3.57 percentage points over CNN-QSVM approaches [22] for 4-class diagnostic tasks. The performance gains stem from key architectural innovations validated by the experimental results: feature preservation strategies, enhanced quantum encoding approaches, and adaptive fusion mechanisms. These design choices enable the detection of complex morphological patterns while maintaining practical computational requirements for clinical deployment.

The maintained performance under realistic NISQ noise conditions (>99% accuracy with comprehensive error modelling) demonstrates deployment readiness superior to previous simulation-only validations. The robust 4-class diagnostic capability addresses clinical staging requirements that binary classification approaches cannot fulfil, providing practical advancements for real-world neuroimaging applications where accurate disease progression assessment is essential for treatment planning. The results validate the quantum frequency-domain processing approach for medical imaging, demonstrating that quantum circuits can provide tangible computational advantages in pattern recognition tasks. The integrated methodology establishes a foundation for quantum-enhanced medical imaging systems that can operate effectively within current technological constraints while providing clinically meaningful diagnostic improvements.

TABLE V. COMPARATIVE PERFORMANCE OF HYBRID QUANTUM–CLASSICAL ALZHEIMER'S CLASSIFICATION METHODS ON MRI

Study	Year	Dataset Size	Architecture	Task	Accuracy (%)	Precision	Recall	F1-Score	AUC
QCNN – Kaggle	2025	5 121 (Kaggle)	6-qubit QCNN + QFT	4-Class	95.71	0.95	0.95	0.95	0.9954
QCNN – OASIS	2025	20 000 (OASIS)	6-qubit QCNN + QFT	4-Class	99.58	1.00	1.00	1.00	0.9997
Modified QResNet18 – Kaggle	2025	5 121 (Kaggle)	6-qubit QResNet18 + QFT	4-Class	97.56	0.94	0.94	0.94	0.9969
Modified QResNet18 – OASIS	2025	20 000 (OASIS)	6-qubit QResNet18 + QFT	4-Class	99.67	1.00	1.00	1.00	1.0000
[33]	2022	6 400 (balanced binary)	ResNet34 → 4-qubit VQC	2-Class	97.20	0.972	0.972	0.972	–
[19]	2023	5 438 (ADNI; binary)	ResNet18 → 4-qubit VQC	2-Class	97.50	–	–	–	–
[20]	2023	6 400 (ADNI/PPMI; binary)	AlexNet → 4-qubit VQC	2-Class	96	–	–	–	–
[21]	2024	40 384 (Kaggle; 4-Class MRI)	ViT + 4-qubit VQC	4-Class	84.3	–	–	–	0.8667
[22]	2024	≈ 50 000 (ADNI + NIFD)	CNN + PCA → 8-qubit QSVM	4-Class	96.1	–	–	–	–

4.7 Clinical Implications and Deployment Considerations

The exceptional very mild dementia detection accuracy (99.86% on OASIS by modified QResNet18) addresses critical clinical needs for early intervention capabilities. The quantum frequency-domain processing paradigm showed remarkable performance in early-stage classification tasks, achieving very good accuracy on very mild dementia detection. While such results suggest clinical promise, validation in real clinical settings and comparison with current diagnostic protocols are needed to establish clinical utility. The multiprotocol versatility exhibited through coronal (Kaggle) and axial (OASIS) orientations provides real-world deployment flexibility through a variety of clinical imaging contexts. Axial slices performed better than coronal slices did, which contradicts typical clinical protocols when examining the hippocampus. This finding indicates that quantum processing can identify useful patterns in the global brain structure that traditional spatial methods overlook. From a computational efficiency viewpoint, the custom QCNN trains on the Kaggle dataset within just 4.02 hours; thus, this approach can provide limited computing resources to hospitals. For research purposes, where maximum accuracy is essential, the modified QResNet18 has better diagnostic capability.

4.8 Technical limitations and future directions

The use of low-resolution inputs (28×28 pixels) throughout the experiments was a deliberate trade-off to reduce computational demands and facilitate real-time simulation of quantum components. While this resolution retains key structural features for Alzheimer's classification, it may overlook subtle anatomical patterns associated with the earliest stages of the disease. Additionally, despite incorporating realistic quantum noise models, simulation-based validation cannot fully replicate the hardware limitations of existing quantum processors, such as short coherence times, limited qubit connectivity, and gate errors. The current six-qubit configuration represents a practical upper bound for NISQ-era hardware, where noise accumulation and hardware fragility present significant challenges for deeper or wider circuits. Consequently, near-term hybrid architectures are expected to rely primarily on classical feature extraction, with quantum components playing a constrained but complementary role.

Future implementations should focus on architectural optimisation, simplified variational circuits, and qubit-efficient encoding schemes tailored to available hardware platforms. Validation on publicly accessible quantum processors under real noise conditions and hardware constraints will be a crucial step toward deployment. Furthermore, the framework could be extended to other clinical domains where frequency-domain signatures, amplified by quantum processing, may offer diagnostic value—such as in Parkinson's disease or early cognitive impairment. While broader deployment remains contingent on hardware advancements, this study provides a solid foundation for the further development of quantum-assisted medical imaging systems. By explicitly modelling realistic quantum noise and constraining circuit depth, this work supports practical experimentation that aligns with current technological limitations.

5. Conclusion

This study introduces HQC-Net, a hybrid quantum- classical framework for multistage Alzheimer's disease classification via structural MRI. By combining classical convolutional encoders with quantum Fourier-based processing and adaptive attention fusion, the model effectively captures both spatial and frequency-domain features essential for early-stage differentiation. The proposed approach achieved superior accuracy across two benchmark datasets, notably identifying very mild dementia with 99.86% accuracy, which is critical for timely intervention. The integration of quantum encoding and frequency-domain analysis provided tangible diagnostic benefits, particularly in distinguishing morphologically similar stages. Additionally, the model demonstrated adaptability to dataset heterogeneity and clinically relevant imaging variations while remaining computationally feasible on standard resources. Future work may explore simplified implementations on real quantum hardware, optimise the quantum circuit architecture for current NISQ limitations, and examine generalizability across other neurodegenerative conditions. Overall, this work establishes a practical and theoretically grounded foundation for quantum-assisted neuroimaging, highlighting its emerging role in advancing early diagnostic precision. Future studies could further benefit from the use of explainable AI or quantum techniques combined with optimisation methods for feature selection, such as quantum gray wolf optimisation or crow swarm optimisation.

Data availability

The dataset used in this study is publicly available from the Mendeley Data repository at the following link: Alzheimer MRI 4 classes dataset, and OASIS Alzheimer's Detection.

Conflict of interest

The authors declare that there are no conflicts of interest regarding the publication of this paper.

Funding

This research did not receive any specific grant from funding agencies in the public, commercial, or not-for-profit sectors.

Acknowledgement

The authors would like to thank Mustansiriyah University for their valuable support and for providing essential facilities for this research.

Declaration of Generative AI and AI-assisted Technologies in the Writing Process

During the preparation of this work, the authors used ChatGPT (OpenAI) to improve the clarity and readability of the manuscript. After using this tool, the authors reviewed and edited the content as needed and take full responsibility for the content of the publication.

References

[1] W. H. Organization, "Global status report on the public health response to dementia," 2021.

[2] M. Maqsood *et al.*, "Transfer Learning Assisted Classification and Detection of Alzheimer's Disease Stages Using 3D MRI Scans," *Sensors*, vol. 19, no. 11, p. 2645, 2019.

[3] A. Lakhan *et al.*, "FDCNN-AS: Federated deep convolutional neural network Alzheimer detection schemes for different age groups," *Information Sciences*, vol. 677, p. 120833, 2024/08/01/ 2024.

[4] R. Tarawneh and D. M. Holtzman, "The clinical problem of symptomatic Alzheimer disease and mild cognitive impairment," (in eng), *Cold Spring Harb Perspect Med*, vol. 2, no. 5, p. a006148, May 2012, doi: 10.1101/cshperspect.a006148.

[5] S. E. Sorour, A. A. A. El-Mageed, K. M. Albarrak, A. K. Alnaim, A. A. Wafa, and E. El-Shafeiy, "Classification of Alzheimer's disease using MRI data based on Deep Learning Techniques," *Journal of King Saud University - Computer and Information Sciences*, vol. 36, no. 2, p. 101940, 2024/02/01/ 2024.

[6] S. Ul Rehman *et al.*, "AI-based tool for early detection of Alzheimer's disease," *Heliyon*, vol. 10, no. 8, p. e29375, 2024/04/30/ 2024, doi: https://doi.org/10.1016/j.heliyon.2024.e29375.

[7] N. Yamanakkanavar, J. Y. Choi, and B. Lee, "MRI segmentation and classification of human brain using deep learning for diagnosis of alzheimer's disease: A survey," *Sensors (Switzerland)*, Review vol. 20, no. 11, pp. 1-31, 2020, Art no. 3243, doi: 10.3390/s20113243.

[8] G. Zhao, H. Zhang, Y. Xu, and X. Chu, "Research on magnetic resonance imaging in diagnosis of Alzheimer's disease," (in eng), *Eur J Med Res*, vol. 29, no. 1, p. 632, Dec 30 2024, doi: 10.1186/s40001-024-02172-0.

[9] S. Adaszewski, J. Dukart, F. Kherif, R. Frackowiak, and B. Draganski, "How early can we predict Alzheimer's disease using computational anatomy?," *Neurobiology of Aging*, vol. 34, no. 12, pp. 2815-2826, 2013/12/01/ 2013, doi: https://doi.org/10.1016/j.neurobiolaging.2013.06.015.

[10] H. Cui, L. Hu, and L. Chi, "Advances in Computer-Aided Medical Image Processing," *Applied Sciences*, vol. 13, no. 12, p. 7079, 2023. [Online]. Available: https://www.mdpi.com/2076-3417/13/12/7079.

[11] L. K. Avberšek and G. Repovš, "Deep learning in neuroimaging data analysis: Applications, challenges, and solutions," *Frontiers in Neuroimaging*, Review vol. 1, 2022, Art no. 981642, doi: 10.3389/fnimg.2022.981642.

[12] M. Li, Y. Jiang, Y. Zhang, and H. Zhu, "Medical image analysis using deep learning algorithms," (in English), *Frontiers in Public Health*, Original Research vol. Volume 11 - 2023, 2023-November-07 2023, doi: 10.3389/fpubh.2023.1273253.

[13] A. K. K. Don, I. Khalil, and M. Atiquzzaman, "A Fusion of Supervised Contrastive Learning and Variational Quantum Classifiers," *IEEE Transactions on Consumer Electronics*, pp. 1-1, 2024, doi: 10.1109/TCE.2024.3351649.

[14] E. A. Radhi, M. Y. Kamil, and M. A. Mohammed, "Quantum Machine and Deep Learning for Medical Image Classification: A Systematic Review of Trends, Methodologies, and Future Directions," *Iraqi Journal for Computer Science and Mathematics*, Review vol. 6, no. 2, pp. 107-138, 2025, doi: 10.52866/2788-7421.1252.

[15] M. A. Habeeb, Y. L. Khaleel, R. D. Ismail, Z. T. Al-Qaysi, and F. N. Ameen, "Deep Learning Approaches for Gender Classification from Facial Images," *Mesopotamian Journal of Big Data*, Article vol. 2024, pp. 185-198, 2024, doi: 10.58496/MJBD/2024/013.

[16] D. A. Kadhim and M. A. Mohammed, "Advanced Machine Learning Models for Accurate Kidney Cancer Classification Using CT Images," *Mesopotamian Journal of Big Data*, Article vol. 2025, pp. 1-25, 2025, doi: 10.58496/MJBD/2025/001.

[17] S. M. Ali, A. M. Kadhim, and H. G. Daway, "Heart disease detection using CNN algorithms based on deep learning models," *AIP Conference Proceedings*, vol. 3264, no. 1, 2025, doi: 10.1063/5.0262627.

[18] T. Shahwar *et al.*, "Automated Detection of Alzheimer's via Hybrid Classical Quantum Neural Networks," *Electronics*, vol. 11, no. 5, p. 721, 2022. [Online]. Available: https://www.mdpi.com/2079-9292/11/5/721.

[19] R. Kim, "Implementing a Hybrid Quantum-Classical Neural Network by Utilizing a Variational Quantum Circuit for Detection of Dementia," in *2023 IEEE International Conference on Quantum Computing and Engineering (QCE)*, 17-22 Sept. 2023 2023, vol. 02, pp. 256-257, doi: 10.1109/QCE57702.2023.10231.

[20] N. Alsharabi, T. Shahwar, A. U. Rehman, and Y. Alharbi, "Implementing Magnetic Resonance Imaging Brain Disorder Classification via AlexNet–Quantum Learning," *Mathematics*, vol. 11, no. 2, p. 376, 2023. [Online]. Available: https://www.mdpi.com/2227-7390/11/2/376.

[21] A. Singhal and H. Shah, "QViSTA: A Novel Quantum Vision Transformer for Early Multi-Stage Alzheimer's Diagnosis Using Optimized Variational Quantum Circuits," in *Advancements In Medical Foundation Models: Explainability, Robustness, Security, and Beyond*.

[22] K.-C. Chen, Y.-T. Li, T.-Y. Li, C.-Y. Liu, P.-H. H. Lee, and C.-Y. Chen, "Compressedmediq: Hybrid quantum machine learning pipeline for high-dimensional neuroimaging data," in *2025 IEEE International Conference on Acoustics, Speech, and Signal Processing Workshops (ICASSPW)*, 2025: IEEE, pp. 1-5.

[23] J. Choi *et al.*, "Early-stage detection of cognitive impairment by hybrid quantum-classical algorithm using resting-state functional MRI time-series," *Knowledge-Based Systems*, vol. 310, p. 112922, 2025/02/15/ 2025.

[24] I. Sercek *et al.*, "A new quantum-inspired pattern based on Goldner-Harary graph for automated alzheimer's disease detection," *Cognitive Neurodynamics*, vol. 19, no. 1, p. 71, 2025/05/10 2025, doi: 10.1007/s11571-025-10249-7.

[25] S. Katabathula, Q. Wang, and R. Xu, "Predict Alzheimer's disease using hippocampus MRI data: a lightweight 3D deep convolutional network model with visual and global shape representations," *Alzheimer's research & therapy*, vol. 13, no. 1, p. 104, 2021.

[26] J. Smucny, G. Shi, and I. Davidson, "Deep Learning in Neuroimaging: Overcoming Challenges With Emerging Approaches," (in English), *Frontiers in Psychiatry*, Perspective vol. Volume 13 - 2022, 2022-June-02 2022, doi: 10.3389/fpsyt.2022.912600.

[27] M. A. Nielsen and I. L. Chuang, *Quantum computation and quantum information*. Cambridge university press, 2010.

[28] M. Lubasch, Y. Kikuchi, L. Wright, and C. M. Keever, "Quantum circuits for partial differential equations in Fourier space," *arXiv preprint arXiv:2505.16895*, 2025.

[29] E. Payares and J. C. Martínez, "The enhancement of quantum machine learning models via quantum Fourier transform in near-term applications," *AIP Conference Proceedings*, vol. 2872, no. 1, 2023, doi: 10.1063/5.0163355.

[30] E. Acar, B. Öztoprak, M. Reşorlu, M. Daş, İ. Yılmaz, and İ. Öztoprak, "Efficiency of Artificial Intelligence in Detecting COVID-19 Pneumonia and Other Pneumonia Causes by Quantum Fourier Transform Method," *medRxiv*, p. 2020.12.29.20248900, 2021, doi: 10.1101/2020.12.29.20248900.

[31] J. Preskill, "Quantum computing in the NISQ era and beyond," *Quantum*, vol. 2, p. 79, 2018.

[32] S. Ding, D. He, and G. Liu, "Improving Short-Term Load Forecasting with Multi-Scale Convolutional Neural Networks and Transformer-Based Multi-Head Attention Mechanisms," *Electronics*, vol. 13, no. 24, p. 5023, 2024.

[33] T. Shahwar *et al.*, "Automated Detection of Alzheimer's via Hybrid Classical Quantum Neural Networks," *Electronics (Switzerland)*, vol. 11, no. 5, 2022, doi: 10.3390/electronics11050721.